JMEPEG (2012) 21:2363–2374
DOI: 10.1007/s11665-012-0175-6

1059-9495/$19.00

The Quasi-static Deformation, Failure, and Fracture Behavior of Titanium Alloy Gusset Plates Containing Bolt Holes

Therese Hurtuk, C.C. Menzemer, A. Patnaik, T.S. Srivatsan, K. Manigandan, and T. Quick

(Submitted November 3, 2011; in revised form January 27, 2012)

In this article, the influence of bolt holes, specifically their number and layout on strength, deformation, and final fracture behavior of titanium alloy gusset plates under the influence of an external load is presented and discussed. Several plates having differences in both the number and layout of the bolt holes were precision machined and then deformed under quasi-static loading. The specific influence of number of bolt holes and their layout on maximum load-carrying capability and even fracture load was determined. The conjoint influence of bolt number, bolt layout pattern, nature of loading, contribution from local stress concentration, and intrinsic microstructural effects in governing the macroscopic fracture mode and intrinsic microscopic mechanisms is presented and discussed.

Keywords bolt holes, fracture, gusset plate, microstructure, nature of failure, quasi-static loading, titanium alloy

1. Introduction

Safe and efficient design of connections can be considered to be a critical part of any structural system. In framing systems, a continuous transfer of load from beams or floor systems to girders and columns is often made possible through the use of connections. The involved members can be connected to each other using either a combination of mechanical fasteners or welds. However, at times these connection methods are restricted by: (i) cross section of the structural member involved and (ii) actual construction used in field practice. This has necessitated the need for the use of intermediate members, such as plates, angles, and tees.

Considering the intent of a system's joint, connections can be classified as being either simple or flexible. Simple, or flexible, connections have the intrinsic capability to transfer the reaction shear while concurrently facilitating the occurrence of end rotation of simple beams. On the other hand, rigid or moment connections must aid in the transfer of moment from one member to another structural member. This often demands an adequate level of stiffness from the connections and therefore necessitates the need for more material and added attention. To enable and/or facilitate ease in connection of members to connecting plates, either mechanical fasteners, such as bolts, nuts, and welds, or a judicious combination have been successfully used in a spectrum of structural applications. The mechanical fastener can aid in transferring the load in several different ways depending on how it is used: (a) tension, (b) shear, (c) friction, or (d) a combination of tension and shear. The hangar-type connection is one of the few examples of direct tension. Transfer of load by "direct" shear in mechanical joints often occurs by bolt bearing. The force often tends to act in a plane that is perpendicular to the axis of the bolt, thereby enabling in transfer of the load by shear between the connection plates till such time the bolt slips and bears against the edge of the bolt hole. This often used bearing connector is considered to be flexible and transfers shear only. In this article, we focus on presenting the results of our recent study on simple bolted connections that aid in transferring the load by bearing.

Simple bolted connections can be classified into three types as shown in Fig. 1. Gusset plates often find selection and use at joints where two or more axially loaded longitudinal members intersect. Transfer of the "axial" load would tend to induce a combination of bending, shear, and normal stress in the gusset plate. Secondary stresses due to out-of-plane movement are often neglected, since application of the load is assumed to be symmetric to the plane of the plate and the sandwich-like detail restricts the occurrence of movement. A gusset plate often encounters bending stresses in a manner similar to a deep beam. Consequently, a stress analysis based on elementary beam mechanics is generally not recommended and used. Typical examples of gusset plate include the following: (i) roof and bridge truss joints, (ii) frame bracing connections, and (iii) other members requiring an in-plane connector.

A bolted connection often requires careful consideration of several limit states. This is in addition to the limit states prevalent on the basic member. At the joint, it is essential that both the member and the connection must resist the following: (i) yielding on the gross section, (ii) rupture on the root section, and if possible (iii) the occurrence of block shear. Further, tear-out of the bolt and localized bearing stresses arising from the bolt rubbing against the material are secondary limit states that can occur concurrently and thereby influence the primary limit

Therese Hurtuk, C.C. Menzemer, and **A. Patnaik**, Department of Civil Engineering, The University of Akron, Akron, OH 44325; **T.S. Srivatsan** and **K. Manigandan**, Department of Mechanical Engineering, The University of Akron, Akron, OH 44325; and **T. Quick,** Department of Geology, The University of Akron, Akron, OH 44325. Contact e-mail: tsrivatsan@uakron.edu.

state. Shear rupture may also occur when the connections used are only a single row and often longer than two bolts. Block shear is both a yielding limit and fracture limit state that tends to occur in compact connections that have been fastened using high strength bolts. In essence, depending on strength of the material chosen for the element the failure paths can take on different patterns. However, most failures will tend to resemble a rectangular block of material tearing out along both the tension plane and the shear plane. Block shear is also favored to occur both at and along the periphery of a weld in welded connection. In this article, we present and discuss the load-carrying capability, response and failure of bolted gusset plates made from a titanium alloy.

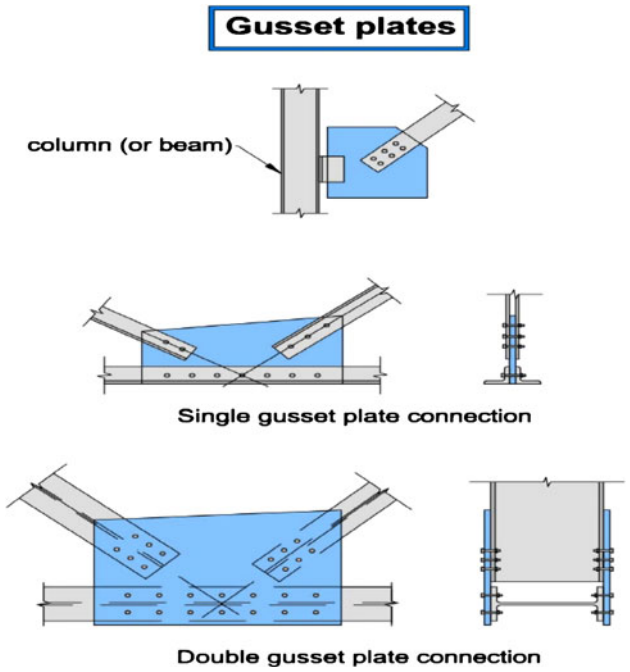

Fig. 1 Types of bolted connections used in structural applications

2. Material

Titanium and its alloys are chosen and used because of their light weight, high stiffness, high strength, and improved corrosion resistance (Ref 1-3). The material chosen for this research study was the widely preferred and chosen titanium alloy, often referred to as the "workhorse" alloy, i.e., Ti-6Al-4V. The alloy used in this specific research study was provided by both TIMET (Wentzville, MO, USA) and ATI Wah Chang (Albany, OR, USA). The primary advantage in choosing this alloy for a structural application is that it is comparatively easy to produce coupled with good hot workability and the relative ease of its receptiveness to heat treatment. The alloy was provided by both the manufacturers in the fully annealed condition. The nominal chemical composition of the alloy provided by the two manufacturers is summarized in Table 1. Uniaxial tensile properties of the alloy, along both the longitudinal and the transverse orientations, are summarized in Table 2.

3. Mechanical Testing

Loading of specimens of the titanium alloy gusset plate was performed on a universal test machine (Model: Warner Swasey) having a 300 kip capacity load cell. Steel test fixtures having a thickness of 25 mm were attached to the test machine. The top fixture, bottom fixture, and test fixture bearing plates were placed in pairs, which facilitated in sandwiching the 6.25 mm thick test specimen while concurrently minimizing loading. The bearing plates that were placed both at the top and at the bottom utilized a 6.25 mm filler to ensure alignment. A schematic of the test set-up is shown in Fig. 2. The top and bottom fixture

Table 1 Nominal chemical composition of the titanium alloy plate material

		Elements							
Lot	**Obtained**	**Ti**	**Fe**	**V**	**Al**	**C**	**O**	**N**	**H**
No. 1	ATI Wah Chang	90.0	0.40	4.00	6.0	0.10	0.20	0.05	0.02
No. 2	TIMET	Balance	0.16	4.05	6.24	0.019	0.18	0.007	…

Lot #1 provided by ATI Wah Chang (Albany, OR, USA) and Lot #2 provided by TIMET (Wentzville, MO, USA)

Table 2 Room temperature tensile properties of Ti-6Al-4V titanium alloy plates

		Elastic modulus		Yield strength		UTS				
Material	**Orientation**	**msi**	**GPa**	**hsi**	**MPa**	**ksi**	**MPa**	**Elongation GL = 0.5", %**	**Reduction in area, %**	**Tensile ductility $\ln(A_o/A_f)$, %**
Ti-6AI-4V	Longitudinal	18	126	137	948	154	1060	7.8	23.8	27.0
	Transverse	20	137	152	1047	171	1181	11.5	21.7	25.0

Results are mean values based on duplicate tensile tests]

pairs served as lap plates in a symmetric butt joint. The symmetry of the two shear planes from this type of connection ensured that a uniaxial load was applied to the test specimen. In essence, the connection is a single gusset plate attached in a manner similar to Fig. 2.

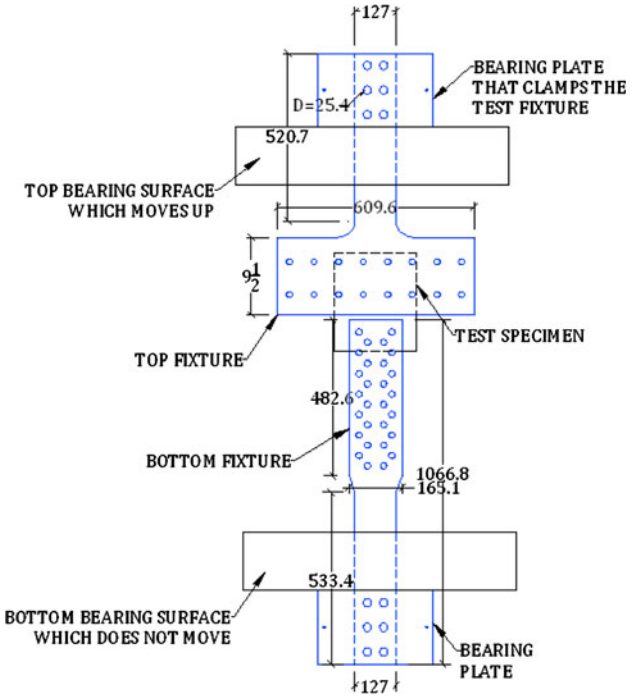

Fig. 2 A schematic of the test set-up that is mounted onto the Universal Test Machine

All the nine plates of the Ti-6Al-4V alloy were loaded at a constant rate of 500 lb/s to ensure quasi-static loading condition. A number of strain gages were mounted on the specimens. Corresponding strains were measured and manually recorded at intervals of 500, 1000, and 2500 lb using a data acquisition system. These intervals were used at different times during the test with increments become smaller as the test progressed.

4. The Test Specimen

The first six specimens or plates were prepared with precision from Lot #1 of the Ti0-6Al-4V alloy plate material provided by ATI (Allegheny Technologies Inc., Pittsburgh, PA, USA) Wah Chang (based in Albany, OR, USA). This is shown in Fig. 3. The gusset plate specimens having the desired bolt pattern were precision machined using a carbide spade drill. The plates were loaded parallel (or longitudinal) to the rolling direction. The remaining four specimens were prepared from Lot #2 provided by TIMET (based in Wentzville, MO, USA). This is shown in Fig. 4. The plate cuts and holes in these plates were precision machined using a water-jet having a precision of 0.005 in. This was followed by careful deburring of the hole.

Design of specific test geometry of the test specimen was influenced by the following:

(a) Size of the plate material available.
(b) Locations of the bolt hole on the test fixture.
(c) Loading capacity of the test machine, and
(d) Strength of the titanium alloy plate.

A width of 12 in. (300 mm) and length of 16 in. (400 mm) was found to be adequate for most of the gusset plates.

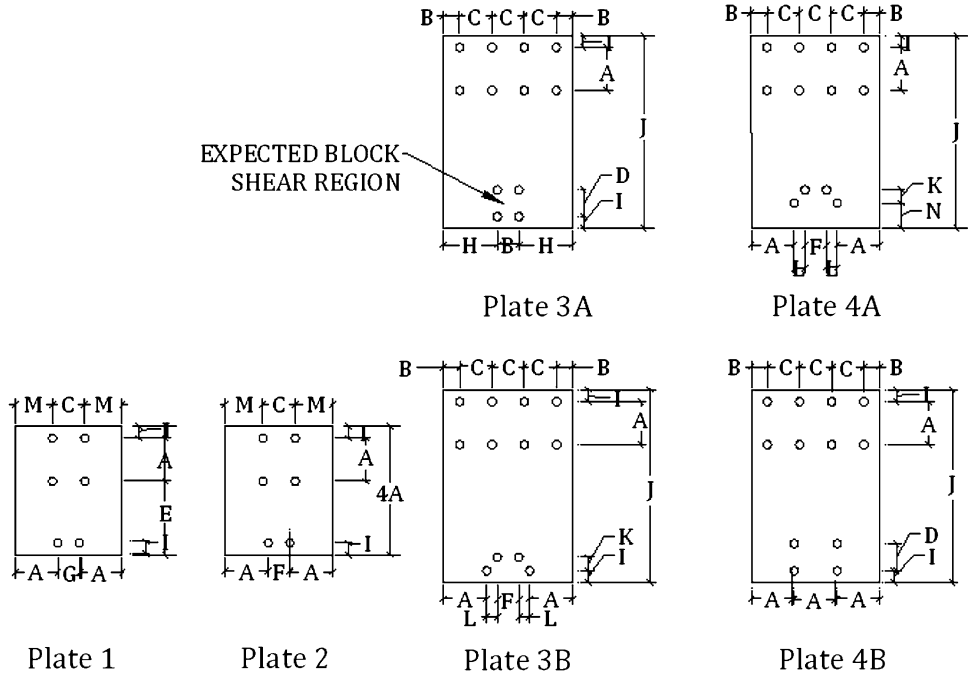

Fig. 3 Geometry and configuration of the titanium alloy plates prepared from Lot #1 of the Ti-6Al-4V alloy provided by ATI Wah Chang (Albany, OR, USA). A: 101 mm, B: 38 mm, C: 76 mm, D: 64 mm, E: 406 mm, F: 51 mm, G: 508 mm, H: 127 mm, I: 28.6 mm, J: 457 mm, K: 32 mm, L: 32 mm, L: 25 mm, M: 89 mm, N: 60 mm

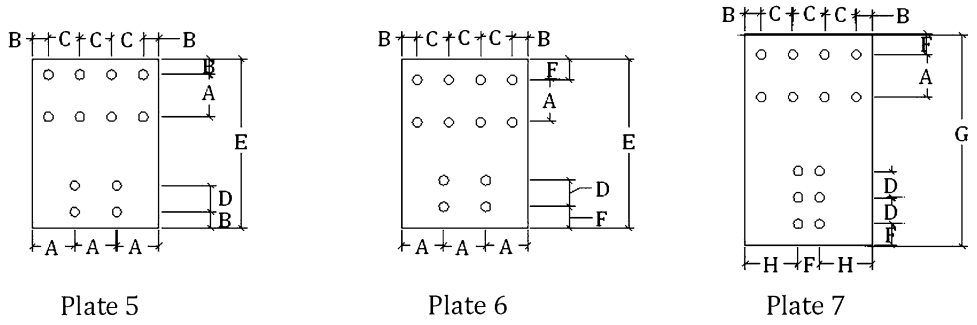

Fig. 4 Geometry and configuration of the test specimens prepared from Lot #2 of the Ti-6Al-4V alloy plate provided by TIMET (Wentzville, MO, USA). A: 101 mm, B: 38 mm, C: 76 mm, D: 64 mm, E: 406 mm, F: 51 mm, G: 508 mm, H: 127 mm, I: 28.6 mm, J: 457 mm, K: 32 mm, L: 32 mm, L: 25 mm, M: 89 mm, N: 60 mm

However, in actual practice the gusset plates are often wider to facilitate accommodating additional member connections. It was believed that a width of 12 in. (300 mm) would not interfere with results of the block shear test. Locations of the bolt holes in the test fixture limited the gage to be either 50 or 100 mm and the pitch to be:

(i) 63.5 mm for the rectangular bolt patterns, and
(ii) 32 mm for the staggered bolt pattern.

Based on predictions of strength, a three-row bolt pattern having a gage of 50 mm was used as the limit for connection length. Plates that were thicker than 6.25 mm were found to be too strong for the test machine. Since diameter of the holes in the test fixture were 19 mm (0.75 in.) it limited the hole in the machined test specimen to be the same size.

High strength A490 bolts were chosen for the tests. A higher load-carrying capability of the material chosen for the bolt minimized and/or eliminated the occurrence of failure of the bolts by shear during testing. A shank having adequate length was chosen for the butt joints such that threads were excluded from the shear plane, thereby maximizing the capacity of the bolt. The bolts were installed snug-tight and upon initial transfer of load, the connection was expected to slip into bearing in the elastic range. The bolt holes in the plate machined from Lot #1 were drilled to 21 mm for placement. All the holes in the plates machined from Lot #2 were water-jet to an oversize of 22 mm.

Using the AISC steel design specification for Block Shear and other limit states, an appropriate choice for both fastener patterns and edge distances were chosen (Ref 4). Geometry of the bolt holes was optimized such that all other potential failure modes, to include shear failure of the bolt, and tensile rupture of the net section would never be reached. Data collection for each test specimen included (a) the applied load, and (b) strains, at specific locations on each test sample. The strain measurements were made using a micro-measurements data acquisition unit (Model: VISHAY 5000). Uniaxial strain gages (Type: CEA-06-125UW-120) were carefully glued onto the titanium alloy plate at selected points for the purpose of measuring strain. Figure 5 shows a biaxial strain gage and its placement and orientation on the plate. Each biaxial strain gage had two numbers; one for the longitudinal strain and one for the transverse strain. Care was taken to ensure that the strain gages were not placed close to the holes where local stress concentration is likely to be the greatest.

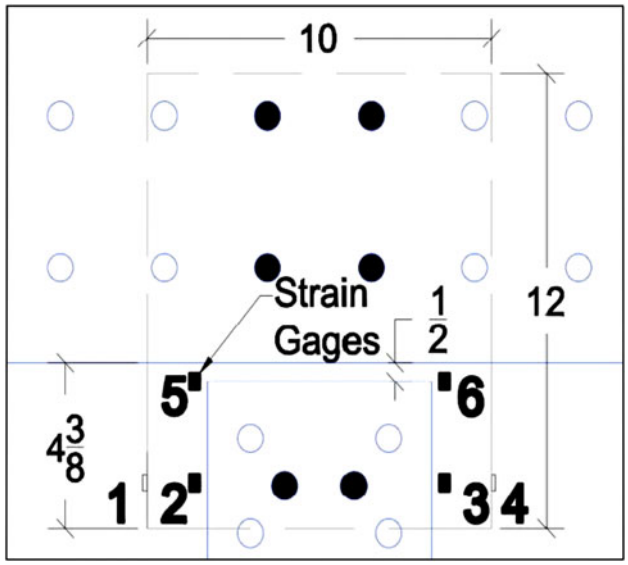

Fig. 5 Schematic showing the placement of strain gages in Plate #1, machined from Lot #1 of the Ti-6Al-4V alloy plate

5. Results and Discussion

5.1 Initial Microstructure

The microstructure of the as-provided material is an important factor that governs its response to an external load or mechanical stimulus. In essence, the microstructure governs the tensile properties, fracture toughness, compressive response, fatigue resistance, and even the kinetics of fracture occurring at both the macroscopic and the microscopic level. The optical microstructure of the candidate Ti-6Al-4V alloy is shown for Plate #5 (Fig. 6a) and Plate #6 (Fig. 6b). These two figures reveal the as-received, undeformed microstructure of the titanium alloy specifically the (i) volume fraction, (ii) morphology, and (iii) size and distribution of the intrinsic microconstituents through the microstructure. Over the range of magnifications spanning very low to high the polished surface of the titanium alloy sample revealed a duplex microstructure consisting of near-equiaxed alpha (α) and transformed beta (β) phases. The primary near-equiaxed-shaped alpha (α) grains (light in color) were well distributed in a lamellar matrix with transformed beta (dark in color). The presence of trace amounts of aluminum and oxygen in this

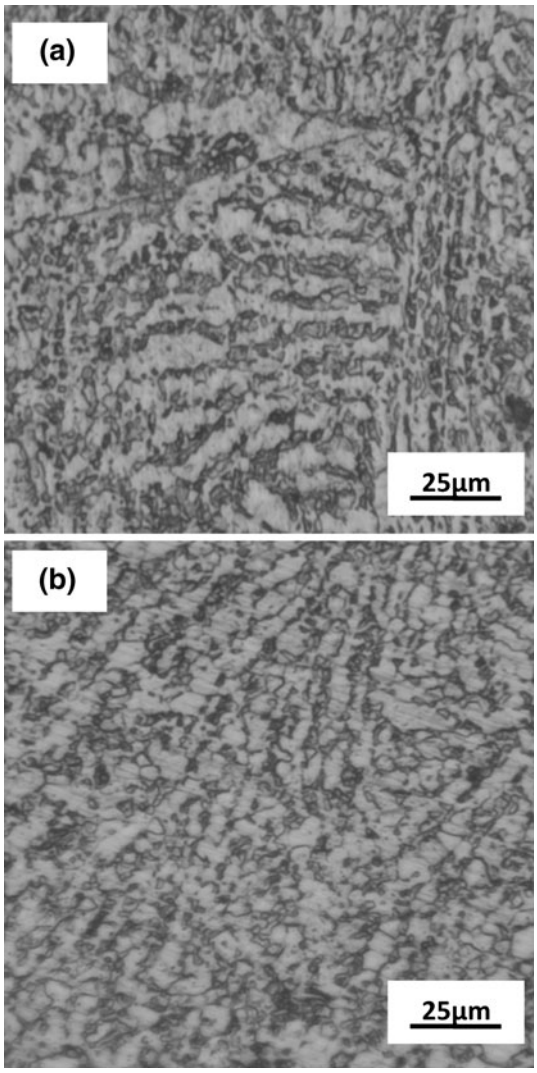

Fig. 6 Optical micrographs showing the key microconstituents in the Ti-6Al-4V alloy (a) Plate #5 and (b) Plate #6

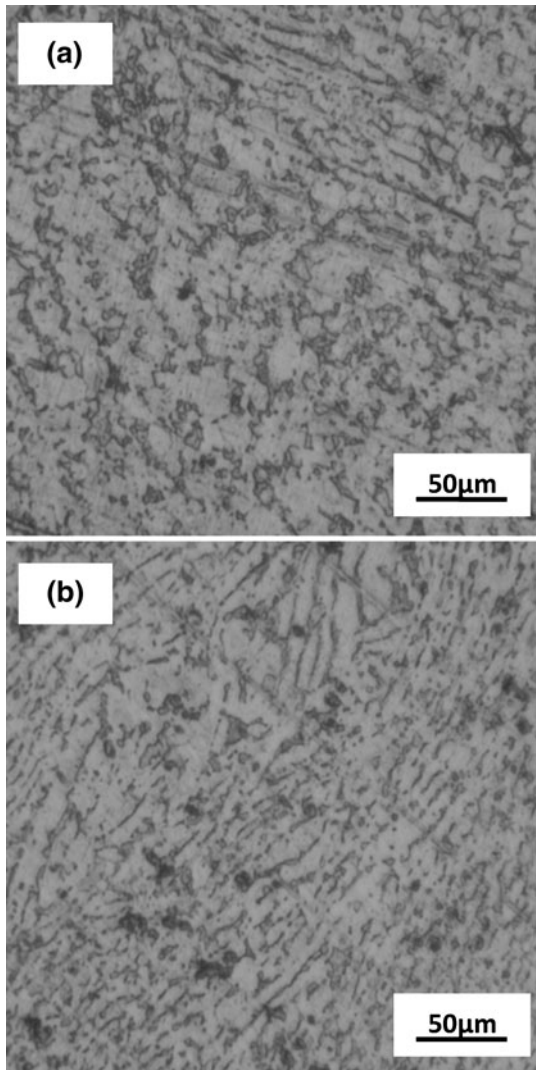

Fig. 7 The key microconstituents, their orientation, and overall dispersion in the Ti-6Al-4V alloy plate: (a) longitudinal plane and (b) transverse plane

Ti-6Al-4V alloy contributes to strengthening and stabilizing the alpha (α) phase, which is beneficial for purpose of (a) enhancing hardenability, (b) increasing strength, and (c) enabling an improvement in response kinetics of the alloy to heat treatment.

The distribution, size, and morphology of the key microconstituents in this alloy along the longitudinal plane of Plate #5 is shown in Fig. 7(a), and the transverse plane of the alloy Plate #5 in Fig. 7(b). A triplanar optical micrograph showing the size, orientation, and morphology of the microconstituents along the three orthogonal directions of the rolled plate is shown in Fig. 8.

5.2 Influence of Loading on Failure of the Titanium Alloy Gusset Plate

Nine gusset plates of the Ti-6Al-4V alloy were designed and tested to fail in block shear. The predominantly observed failure for the mechanically deformed gusset plates was block shear, though other failure modes were also evident. The observed failure modes to include a combination of block shear and others helped provide a better understanding of the influence of applied load on mechanical behavior of the Ti-6Al-4V alloy gusset plate.

Plate #1 (Fig. 9) and Plate #2 (Fig 10) were observed to rupture essentially along the tension plane prior to rupture by fast fracture along the edges of the plate. Failure of both these pates occurred rapidly and without much warning. In considering the observed failure modes of steel gusset plates and aluminum alloy gusset plates in earlier studies (Ref 5-8), the observed failure of the Ti-6Al-4V alloy gusset plates under the influence of an external load is as expected. Under conditions of load-controlled testing, the observed failure load coincided well with the maximum load applied to the gusset plate.

Plate #1 experienced normal tensile rupture between the bolt holes followed by diagonal shear rupture towards the edges. While the observed failure of Plate #2 was identical, the path followed was noticeably different. Tension rupture occurred between the holes located at the bottom. Subsequent rupture towards the left side of loading was curved in a vertical direction, i.e., along the load axis, and rapidly extended to the edge of the plate. These two plates revealed visible signs of

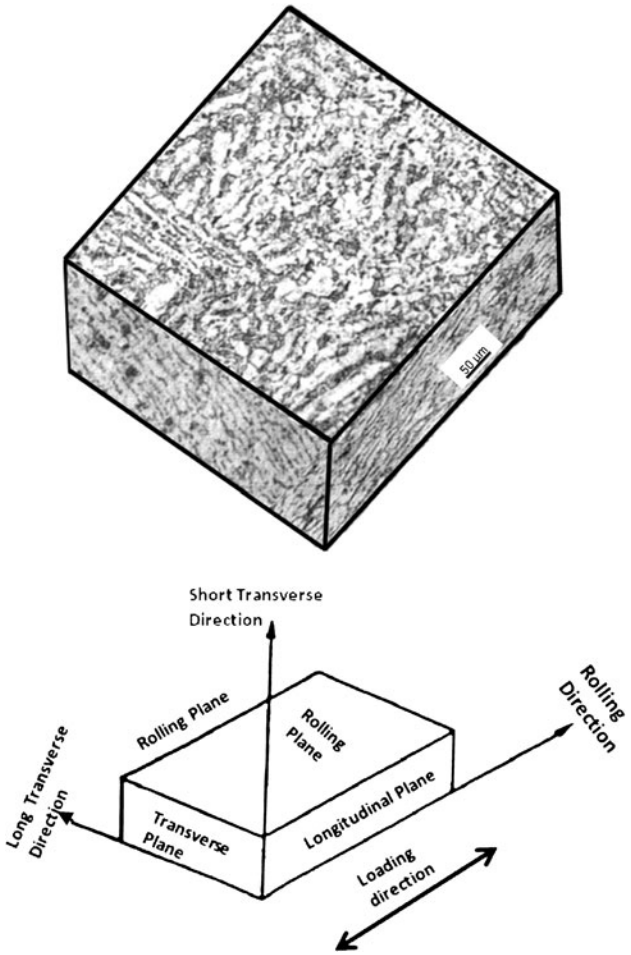

Fig. 8 Triplanar optical micrograph illustrating the microstructure of the Ti-6Al-4V alloy plate along the three orientations: longitudinal, transverse, and rolling planes

Fig. 9 Low-magnification micrograph showing overall morphology of failure of Plate #1

yielding prior to failure with the greatest yielding evident for Plate #2 indicative of the occurrence of the ''orange-peel'' effect. Also, for Plate #2 bulging was evident along the bottom of the plate. This evidence of permanent deformation is ascribed to be due to local compressive yielding, or bearing stresses, caused by the bolts against the holes. The maximum strength of Plate #1 was 390 kN (87 kips) and occurred at the time of failure. The maximum strength of Plate #2 was 401 kN (89.54 kips) and occurred immediately prior to failure [at 374 kN (83.5 kips)].

Fig. 10 Low-magnification micrograph showing overall morphology of failure of Plate #2

Plate #3A of the Ti-6Al-4V alloy revealed failure to be clean and predominantly by ductile block shear. The tension plane ruptured along the net area while the gross area outside of the bolts ruptured by shear. The maximum sustaining load for this plate was 748 kN (167 kips) prior to the occurrence of failure at 681 kN (152 kips). As expected, the tension plane was the first to fracture. The occurrence of ''localized'' deformation due to bearing stresses was noticeably evident.

Plate #3B and Plate #4A both failed by block shear. For both these plates, net section rupture occurred on the tension plane, while shear plane rupture occurred along the outside of the holes, i.e., the gross area, and essentially along a straight path. Bearing stress-induced localized deformation was apparent near all the bolt holes. These two plates reached the maximum load at the time of failure. Plate #3B reached a maximum load of 598 kN (133.5 kips) prior to failure, while Plate #4A reached a maximum load of 757 kN (169 kips) prior to failure.

Failure of Plate #4B was not by block shear. Upon reaching a maximum load of 811 kN (181 kips) failure occurred. The edge distance of 28.6 mm for this plate was not adequate enough to withstand a tear-out failure mode. Along the line of bolts in the interior there occurred a curved fracture path. There were no visible signs of deformation along the tension plane.

When Plate #5 and Plate #6 were loaded, neither of them failed fully by block shear. Both plates experienced a dual-failure mode of block shear and net section rupture. Plate #5 with an edge distance of 38.1 mm failed through the left shear plane when a maximum load of 1069 kN (238.6 kips) was reached. Plate #6 with an edge distance of 50 mm failed when a maximum load of 1150 kN (256.6 kips) was reached with the occurrence of localized bearing stress deformation with little contribution from the shear plane.

Plate #7 had three rows of bolts and can be categorized as the one having the longest connection. This plate when loaded did not fail totally by block shear as compared with Plate #3A. Instead it exhibited a dual-failure mode quite similar to Plate #5 and Plate #6. Localized deformation occurred both at and near the edges of the bolt holes with evidence of minimal yielding on the shear planes.

5.3 A Comparison of Strength (Experimental vs. Theoretical)

The values of experimentally determined strength are compared with the corresponding theoretical value. The theoretical value was calculated using the expression that is used to design block shear in steel:

Table 3 A succinct compilation of theoretically determined and experimentally obtained values of strength of the Ti-6Al-4V alloy gusset plates

Plate	Theoretical value		Experimental value		Theoretical professional factor
	kN	kips	kN	kips	PF
Plate #1	326.6	72.9	389.8	87.0	1.19
Plate #2	326.6	72.9	401.0	89.5	1.23
Plate #3A	649.6	145	748.2	167.1	1.15
Plate #3B	518.8	115.8	598.1	133.5	1.15
Plate #4A	757.1	169.0	757.1	169.0	1.00
Plate #4B	931.8	208.0	811.0	181.0	0.87
Plate #5	1008.0	225.0	1068.9	238.6	1.06
Plate #6	1106.6	247.0	1149.6	256.6	1.04
Plate #7	1097.6	245.0	1298.8	289.9	1.18

Professional factor defined as ratio of experimental value to the theoretical value

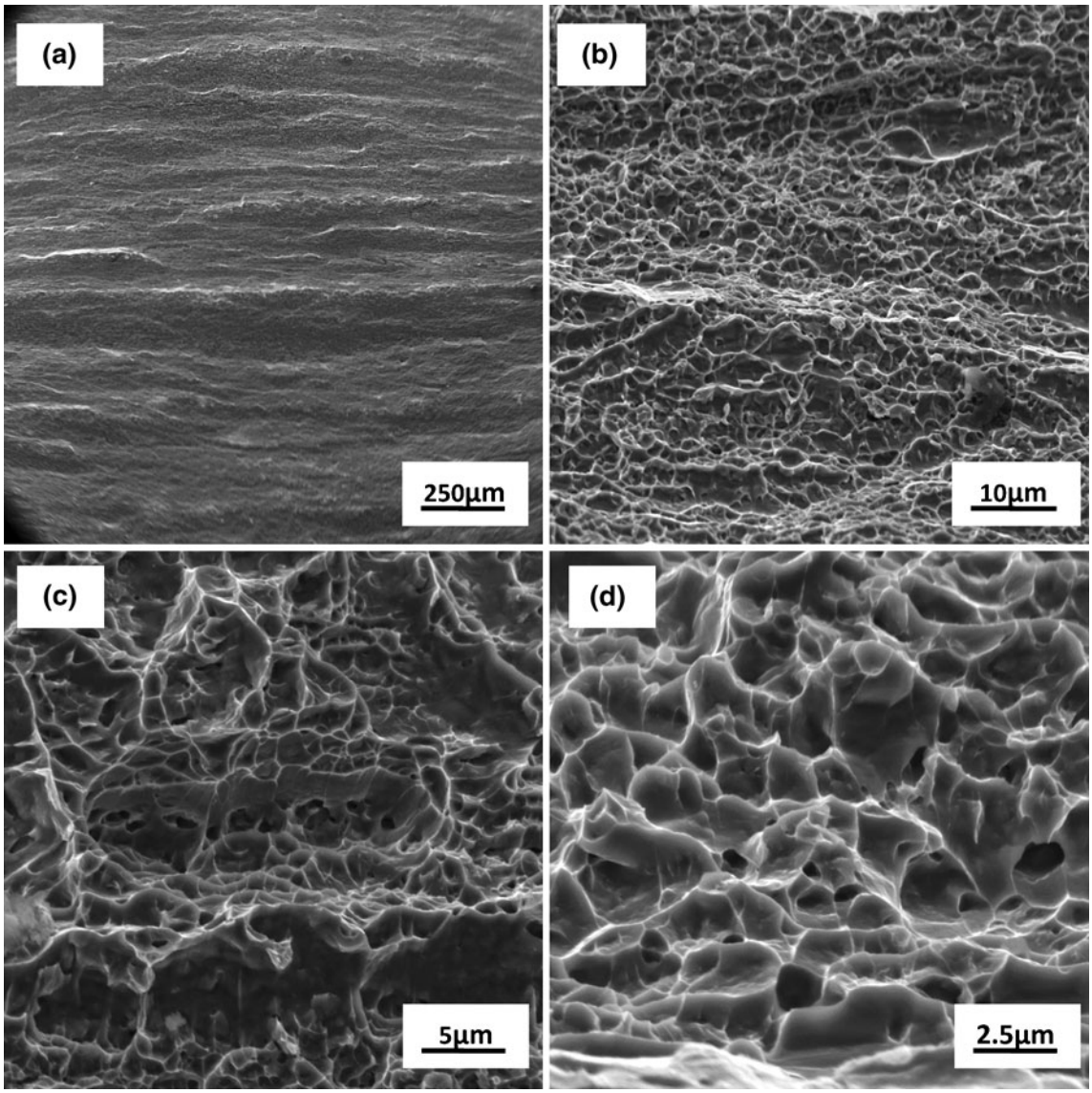

Fig. 11 Scanning electron micrographs of the deformed and failed Ti-6Al-4V plate **(**Plate #5) at the section of the grip showing: (a) overall morphology of failure, (b) high-magnification observation of (a) showing a sizeable population of ductile dimples, (c) high magnification observation of (b) showing the size, nature, and morphology of dimples interdispersed with fine microscopic voids, and (d) healthy population of dimples and isolated and randomly spaced microscopic voids on the overload fracture surface

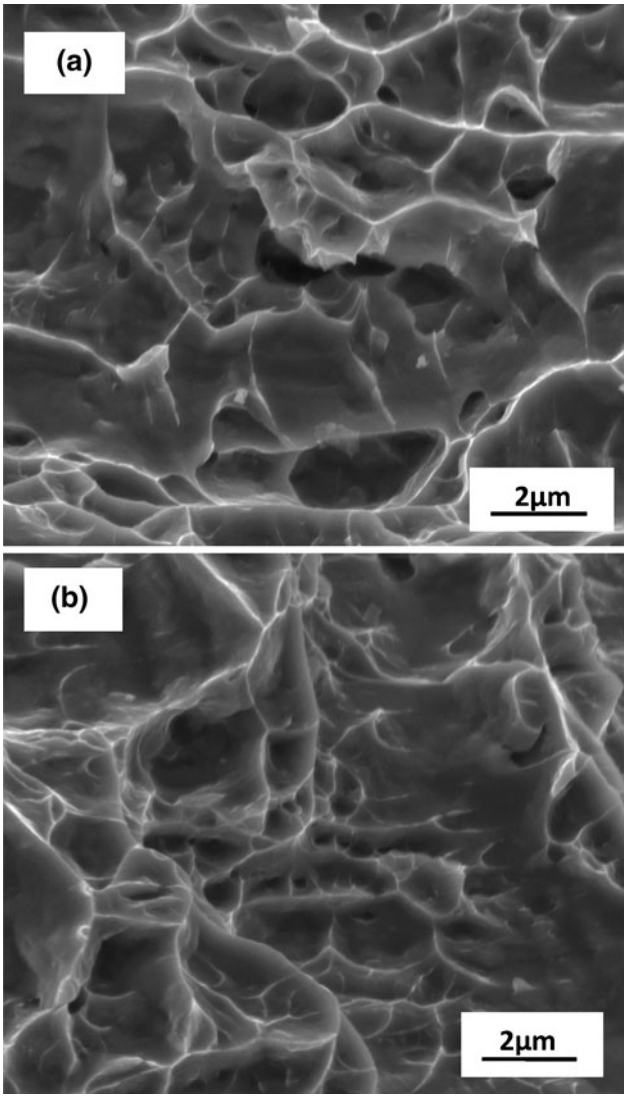

Fig. 12 Scanning electron micrographs of the deformed and failed Ti-6Al-4V plate (Plate No. 5) at the grip section showing: (a) coalescence of the fine microscopic voids to form a microscopic crack and a population of dimples of varying size and shape and (b) the shallow nature of dimples in the region adjacent to crack initiation

$$R_n = 0.6F_uA_{nv} + U_{bs}F_uA_{nt} < 0.6F_yA_{gv} + U_{bs}F_uA_{nt} \qquad \text{(Eq 1)}$$

$$\text{Standard condition: } 0.6\,F_yA_{gv} + F_uA_{nt}$$
$$\text{Shear condition: } 0.6\,F_uA_{nv} + F_uA_{nt}$$

In this expression F_u is ultimate tensile strength of the titanium alloy, F_y is tensile yield strength of the titanium alloy, A_{gv} gross area of shear ligament, A_{nv} net area of shear ligament, A_{nt} net area of tensile ligament, and is U_{bs} is the reduction coefficient.

This equation is representative of the current AISC block shear model for steel (Ref 9, 10). Based on AISC specification for bolt spacing and edge distances, maximum and minimum length of the tension plane and maximum and minimum length of the shear plane coupled with geometric limitations for the gusset plate were determined and this is well-documented elsewhere (Ref 4). The experimental and theoretical values are summarized in Table 3. The two values show a noticeable difference for the entire titanium alloy plates tested. For all plates of this Ti-6Al-4V alloy the theoretical value is marginally less than the experimental value. The difference in the two values is as high as 15 pct. This noticeable difference is ascribed to the role and contribution of intrinsic microstructural effects and the occurrence and presence of "local" stress concentration at the bolt holes in governing the mechanical response of a plate under conditions of experimental tests, i.e., external mechanical stimulus. The effects and/or contribution of intrinsic microstructural effects in synergism with the presence of "local" stress concentration at the bolt holes is not taken into consideration for strength calculations using Eq 1. The intrinsic influence of microstructure and local stress concentration can be partially understood by examining the fracture surfaces of the deformed and failed plates. Only representative fracture surface features observed for Plate #5 and Plate #6 are presented and discussed.

5.4 Fracture Behavior of the Deformed Titanium Alloy Plates

A careful and comprehensive examination of the fracture surfaces of the deformed and failed specimens of Plate #5 and Plate #6 was done in a scanning electron microscope (SEM) over a range of magnifications. This enabled in establishing the specific role played by the intrinsic microstructural features and intrinsic microstructural effects on strength, ductility, fracture, and overall performance of the Ti-6Al-4V alloy under the influence of loading or an external mechanical stimulus. Representative fractographs of the deformed and failed fracture surface of the plate are shown in Fig. 11 to 13 for Gusset Plate #5 and in Fig. 14 and 15 for Gusset Plate #6.

5.4.1 Fracture Behavior of Gusset Plate #5. At the macroscopic level, failure of the plate was essentially normal to the applied load axis at the global level. Overall morphology of the fracture surface appeared to be rough and layered (Fig. 11a). Observation of the fracture surface at a higher magnification revealed a sizeable population of dimples of varying size and shape (Fig. 11b). At the higher allowable magnifications of the SEM the dimples were found to be interdispersed with fine microscopic voids, features reminiscent of the locally ductile failure mechanisms (Fig. 11c). The overload region of the fracture surface near the grip revealed a noticeable population of dimples and randomly distributed fine microscopic voids (Fig. 11d). At selected locations dispersed through the fracture surface was observed gradual growth and eventual coalescence of the fine microscopic voids to form a fine microscopic crack, coupled with a population of voids of varying size and shape (Fig. 12a). Immediately adjacent to the region of crack initiation and early growth the dimples were shallow in nature and varying in both size and morphology (Fig. 12b).

Electron microscopy observations of the shear region of the fracture surface are shown in Fig. 13. Overall morphology was observably featureless at low magnifications of the SEM (Fig. 13a). Progressive examination at the higher allowable magnifications of the SEM revealed the shear surface to be covered with a sizeable population of dimples reminiscent of locally operating ductile failure mechanisms (Fig. 13b). At gradually higher magnification the size, shape, and morphology of the ductile dimples was clearly evident (Fig. 13c). In the region approaching overload in addition to a sizeable population of dimples was observed coalescence of the fine microscopic voids to form a microscopic crack (Fig. 13d).

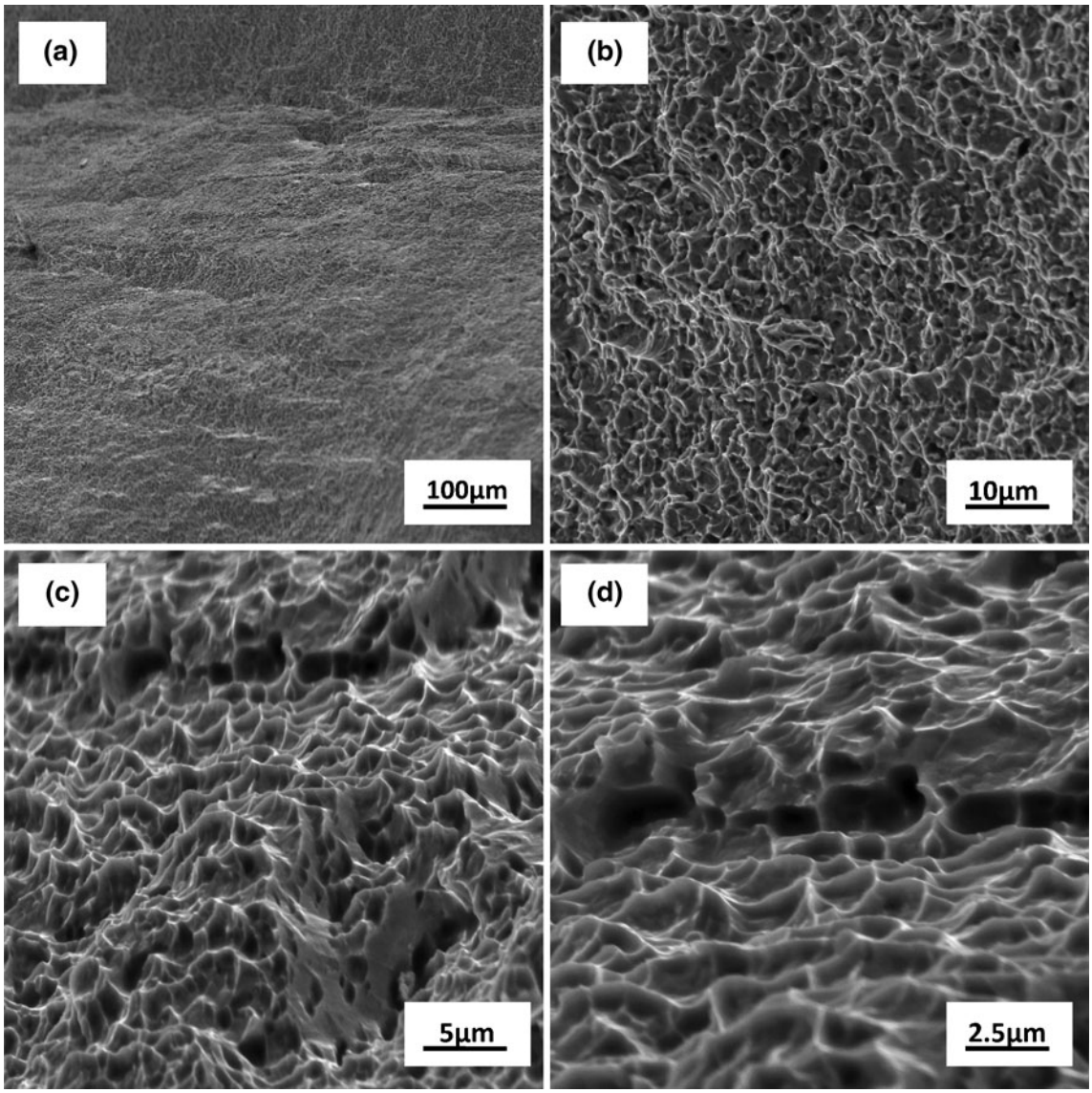

Fig. 13 Scanning electron micrographs of the deformed and failed Ti-6Al-4V alloy plate (Plate #5) at the region and/or location of shear rupture showing: (a) overall morphology of failure in the shear region, (b) high-magnification observation of (a) showing a healthy population of ductile dimples, reminiscent of the locally operating failure mechanism, (c) the size, shape, and morphology of the dimples covering the shear region and microvoid coalescence, and (d) in the region approaching overload the shallow nature of dimples and microscopic void coalescence to form a microscopic crack

5.4.2 Fracture Behavior of Gusset Plate #6. At the macroscopic level, failure of this plate at the section or region closer to the grip was essentially flat and normal to the far-field applied stress axis at the global level. The region immediately adjacent to the onset of damage was flat and covered with an observable population of dimples, reminiscent of the ''locally'' operating ductile failure mechanisms (Fig. 14a). At gradually higher magnifications the dispersion of dimples was found to be intermingled with fine microscopic voids (Fig. 14b). These features are indicative of ductile failure at the fine microscopic level. In the region immediately prior to overload the fracture surface was found to be covered with (i) dimples of varying size, (ii) a noticeable population of fine microscopic voids, and (iii) isolated microscopic cracks (Fig. 14c). Near similar features of voids, dimples, and microscopic cracking were found covering the overload fracture surface (Fig. 14d).

In the shear-dominated region of failure the key micrographs are shown in Fig. 15. Overall morphology of failure was indicative of globally ductile failure (Fig. 15a). Progressive high-magnification observation of the fracture surface revealed clearly the size, morphology, and shallow nature of the dimples (Fig. 15b). In the region immediately prior to overload the key features being voids, dimples, and isolated microscopic crack (Fig. 15c). The shear section of the fracture surface revealed pockets of flat and near featureless regions interdispersed with shallow dimples and isolated microscopic cracks (Fig. 15d).

5.4.3 The Mechanisms Governing Fracture at the Fine Microscopic Level. The occurrence and presence of localized stress intensities at selected points through the Gusset plate during far-field loading, the resultant ''localized'' strain is conducive for the nucleation and concurrent growth of the fine microscopic voids (Ref 11, 12). The enlarged microscopic

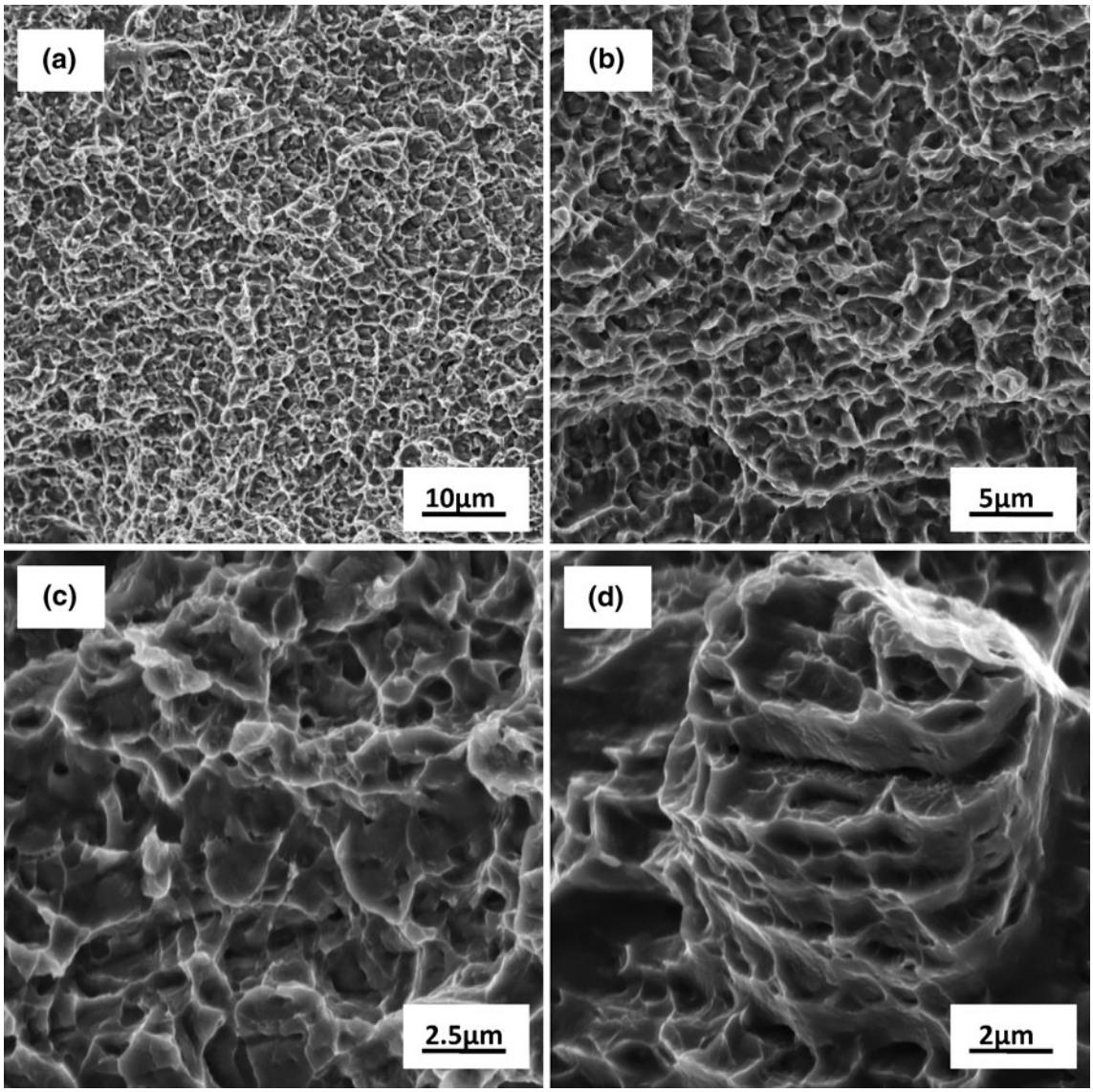

Fig. 14 Scanning electron micrographs of the deformed and failed Ti-6Al-4V alloy plate (Plate #6) at the location of the grip, showing: (a) the region immediately adjacent to initiation of crack at low magnification, (b) high-magnification observation of (a) showing the dispersion of dimples intermingled with fine microscopic voids, (c) the key features on the fracture surface in the region prior to overloads, and (d) voids, elongated dimples, and microscopic cracks in the region of overload reminiscent of locally operating ductile failure mechanism

voids tend to eventually coalescence with each other and with the adjacent microscopic voids. This tends to often occur at low values of the ''local'' stress. The process of initiation, gradual growth, and eventual coalescence by impingement of the microscopic voids with each other and with neighboring macroscopic voids results in the early initiation and the presence of very fine microscopic cracks. These cracks were observed to be randomly distributed through the fracture surface. The halves of these macroscopic voids and fine microscopic voids are the shallow dimples, of varying size, distinctly visible and spread through the fracture surface.

With continued loading and resultant increase in the ''local'' stress intensity the fine microscopic cracks are favored to gradually grow through the alloy microstructure and eventually become a macroscopic crack. The macroscopic crack is favored to propagate in the direction of the major stress axis.

6. Conclusions

Based on a comprehensive study of the mechanical response of titanium alloy gusset plates when subject to an external mechanical stimulus culminating in its failure by fracture following are the key observations:

1. Polished surface of the titanium alloy sample revealed a duplex microstructure consisting of near-equiaxed alpha (α) and transformed beta (β) phases. The primary near-equiaxed-shaped alpha (α) grains were well distributed in a lamellar matrix with transformed beta (β).
2. Rupture of a titanium alloy gusset plate in tension always occurred on a net area quite similar to failure of other metals used for gusset plates, such as aluminum alloys

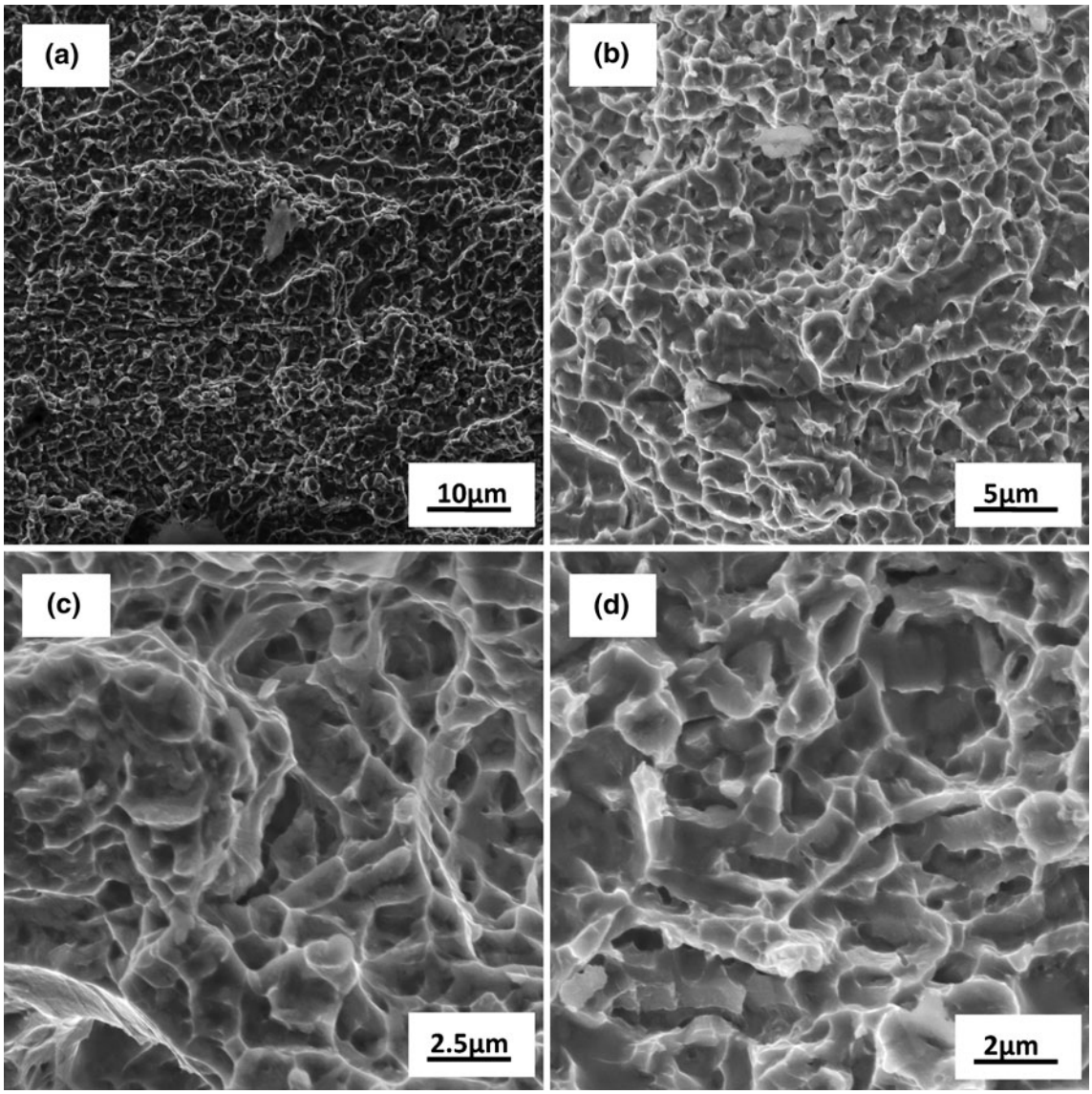

Fig. 15 Scanning electron micrographs of the deformed and failed Ti-6Al-4V alloy plate (Plate #6) at the location of shear failure showing: (a) overall morphology of failure at the region, (b) high-magnification observation of (a) showing the size, morphology, and shallow nature of dimples, (c) in the region immediately prior to overload the key features being voids, dimples, and isolated microscopic cracks, and (d) pockets of flat and near featureless regions intermingled with shallow dimples in the region of shear failure

and steel, by block shear. Under conditions of load-controlled testing the observed failure load coincided well with the maximum load applied to the gusset plate.

3. Stress development and resultant deformation that occurred on the shear plane is a function of ductility of the titanium alloy, length of the shear plane and width of the tension plane. Plates having the width of the tension plane to be 200 mm did not fail by block shear. This gage prevented the development of stress on the shear plane.
4. For all gusset plates of this Ti-6Al-4V alloy that were subject to an external mechanical stimulus or load the theoretical value is marginally less than the experimental value. The difference between the two values was as high as 15%. This noticeable difference is ascribed to the synergistic influences of the role and contribution of intrinsic microstructural effects coupled with the presence of "local" stress concentration at the bolt holes in governing the mechanical response of a plate under conditions of experimental tests.
5. For those titanium alloy gusset plates that had a longer shear connection, the shear plane was resistant to the development of stress causing failure to occur elsewhere. Overall mode of failure was a combination of block shear and tensile rupture of the net section.
6. Overall strength of bolted connections of this titanium alloy gusset plate against block shear was good. This in combination with the non-corrosive nature of this titanium alloy, i.e., Ti-6Al-4V, makes it a potentially viable and functionally attractive replacement for steel as a material for gusset plates.
7. Overall failure of the plate was essentially normal to the applied load axis at the global level. SEM revealed the shear surface to be covered with a sizeable population of

dimples of varying size. Region immediately adjacent to the onset of damage initiation was flat and covered with a noticeable population of dimples, reminiscent of the "locally" operating ductile failure mechanisms. The gradual growth and eventual coalescence by impingement of the fine microscopic voids with each other and with neighboring macroscopic voids resulted in early initiation and the presence of fine microscopic cracks. These cracks were randomly distributed through the fracture surface. The halves of these macroscopic voids and fine microscopic voids are the shallow dimples.

References

1. M.J. Donachie, Jr., *Titanium a Technical Guide*, 2nd ed., ASM International, Metals Park, 2000, p 1–15
2. F.H. Froes, Titanium, *Encyclopedia of Materials Science and Engineering*, P. Bridenbaugh, Ed., Elsevier, Oxford, 2000,
3. F.H. Froes, Titanium Metal Alloys, *Handbook of Chemical Industry Economics*, J. Ellis, Ed., Wiley, New York, 2000,
4. T.M. Hurtuk, Investigating and Understanding the Behavior of Titanium Alloy Gusset Plate under Block Shear, Master of Science Thesis, The University of Akron, August 2011
5. S.G. Hardash and R. Bjorhovde, New Design Criteria for Gusset Plates in Tension, *AISC Eng. J.*, 1985, **22**(2), p 77–94
6. B.B.S. Huns, G.Y. Grondin, and R.G. Driver: *Block Shear Behavior of Bolted Gusset Plates*, Structural Report No. 248, Department of Civil and Environment Engineering, University of Alberta, Canada, 2002
7. J.E. May and C.C. Menzemer, Strength of Bolted Aluminum Alloy Tension Members, *J. Struct. Eng.*, 2005, **131**(7), p 1125–1134
8. C.C. Menzemer, L. Fei, and T.S. Srivatsan, Design Criteria for Bolted Connection Elements in Aluminum Alloy 6061, *J. Mech. Des.*, 1999, **121**, p 348–358
8. C.C. Menzemer, L. Fei, and T.S. Srivatsan, Design Criteria for Bolted Connection Elements in Aluminum Alloy 6061, *J. Mech. Des.*, 1999, **121**, p 348–358
9. American Institute of Steel Construction (AISC), *Specifications for Structural Steel Buildings, Unified 13th edition*, AISC, Chicago, IL, 2005
10. American Institute of Steel Construction (AISC), *Specifications for Structural Steel Buildings, Unified 14th edition*, AISC, Chicago, IL, 2010
11. T.S. Srivatsan and M. Kuruvilla, *Microstructure, Hardness, Tensile Deformation, Cyclic Fatigue and Fracture Behavior of Ti-Al-V-Fe-O Alloy: Role of Sheet Stock*, Final Technical Report, ATU Wah Chang, March 2007
12. U. Bathini, T.S. Srivatsan, A. Patnaik, and T. Quick, A Study of the Tensile Deformation and Fracture Behavior of Commercially Pure Titanium and a Titanium Alloy: Influence of Orientation and Microstructure, *J. Mater. Eng. Perform.*, 2010, **19**(8), p 1172–1182